Co-operative 2-D inversion of collocated high-resolution seismic, dc resistivity and audiofrequency MT profiles: Application to near-surface bedrock-cover mapping

Max Meju[1], Luis Gallardo[1], Adel Mohamed[2], Emin Ulugergerli[3]. Lancaster University,UK[1]/El-Mansoura University, Egypt[2]/Ankara University, Turkey[3].

Abstract

Seismic, dc resistivity, transient electromagnetic (TEM) and audiofrequency magnetotelluric (AMT) methods have been jointly applied to the characterisation of a complex bedrock and overlying sedimentary rocks in an area covered by heterogeneous glacial deposits in midland England. Maps of TEM voltage response enabled a clear assessment of spatial variability and significant fracture-zones in the complex basement. The TEM sounding curves served for static shift correction of AMT data. Co-operative 2-D regularised inversion of the dc, AMT and seismic data led to concordant models of the subsurface and allowed improved determination of the basement-cover relations in the area of study.

Introduction

Highly portable audiofrequency magnetotelluric (AMT), transient electromagnetic (TEM) and dc resistivity (herein collectively referred to as geoelectromagnetic or GEM) as well as seismic refraction methods are now available for near-surface studies. Also, sophisticated multi-dimensional inverse modelling schemes for interpreting traditional GEM and seismic field data (e.g., *Mackie et al.*, 1997; *Zelt and Barton,* 1998) can be appropriately scaled to handle near-surface imaging problems. It is thus possible to collect high quality, spatially dense measurements along the same survey lines and invert them to determine the resistivity and velocity structure of the near-surface in complex bedrock environements. We have obtained TEM, dc resistivity, AMT and seismic refraction data along coincident profiles at a test site underlain by the Mountsorrel granodiorite in midland England (Figure1).

The Mountsorrel granodiorite (MG) forms the bedrock in Quorn and surrounding areas. This body was unroofed, deeply weathered and eroded during Permo-Triassic times resulting in a highly irregular surface. It was subsequently overlain by the Mercian Mudstone (MM) deposits. Heterogeneous glacial drift deposits form a 1-3 m thick surficial blanket in the area. MG outcrops in the southern margin of the study site (Figure1) and is believed to descend northwards in a step-wise manner under sedimentary cover. It is heavily fractured at outcrop and presumably at depth (based on field observations at the largest hardrock quarry in western Europe located ca. 400 m south of our survey grid). The Quorn site is thus an excellent natural laboratory for assessing the effectiveness of high resolution 2-D imaging surveys for mapping the bedrock and cover sequences. The question we seek to answer using a co-operative 2D data imaging approach is: Can we resolve the geologically suggested step-like structre of the MG basement as well as the resistivity and velocity structure of MM and the glacial cover materials?

Survey Method, Data Analysis and Examples

The Quorn site is a relatively flat grazing ground and topographic heights were available from a previous differential GPS survey using the Magellan 5000 PRO system. Collocated high-resolution TEM, dc resistivity, seismic refraction and AMT surveying were conducted at the site (Meju et al., 2003). The TEM profiling employed the Geonics EM47 system in the central-loop configuration. The measurements used contiguous (20 m-sided) transmitter loops along six N-S survey lines (80E to 20W in Figure 1) and served to pinpoint any spatial variability or significant fracture-zones in the bedrock. Areal maps of the TEM voltage responses for selected time-windows are presented in Figure 2. Notice that the TEM data show spatial variability with significant differences in amplitude between north and south of position 180S. Based on these TEM maps, the best location for collocated GEM and seismic 2D surveying would be near line 20W.

Detailed 2D profiling experiments were conducted on Line 20W (Meju et al., 2003). Bi-directional Schlumberger dc soundings were made at selected positions (ca. 40 m apart) with N-S and E-W expanding electrode arrays (AB/2 of 1.5 to 90 m). Seismic travel-time data were recorded along the line using a Bison multi-channel seismograph with a sledgehammer as energy source and a geophone spacing of 2 m. The source was used at both ends of the profile and at two intermediate points along the line to generate continuous forward and reverse profiles of potential refractors. AMT data were simultaneously recorded in two orthogonal directions in the frequency range 10 Hz to 100 KHz using a station spacing (and electric dipole lengths) of 15 m. The Geometrics Stratagem Model EH4 field system was used for the AMT survey.

Sample dc, TEM and AMT apparent resistivity (ρ_a) data from station 45S on line 20W are presented in Figure 3 using a convenient common-scale [*Meju*, 2002, eq. 1 & 2] in which AB/2 (or *L* in metres) is converted to the equivalent transient time (*t* in msec) using the relation *t* =

$(\pi\mu_0 L^2)/2\rho_a$ where ρ_a is in Ωm and $\mu_0=4\pi\times10^{-7}$ H/m; t is then converted to an equivalent MT frequency. Notice the agreement between the various ρ_a sounding curves. The AMT data are relatively poor in quality and were corrected for static shift using the TEM data from coincident locations (cf. *Sternberg et al*., 1988; Meju 1996).

Method of 2-D Data Inversion

Separate inversion of remotely sensed geophysical data sets is typically bedeviled by non-uniqueness due to a variety of reasons of which measurement errors, nonlinearity of the underlying physical phenomena and geological heterogeneity are the most problematical. Combined or co-operative analysis of data from different methods may reduce the ambiguities in geophysical interpretation. This is the approach adopted in this paper.

The regularised inverse problem here is to reconstruct the smoothest 2D distribution of the relevant physical parameters in the subsurface that explained the field observations to within a preset (1 *rms*) error. Only the in-line (N-S) measurements on line 20W have been inverted to yield 2D images required for the comparability analysis. The in-line AMT data were taken as the TM-mode responses and the noisy sections smoothed before inversion. The dc resistivity data were inverted using the 2D inversion algorithm of Perez-Flores et al., *(*2001). The finite-difference based, conjugate gradient inversion scheme of Mackie et al., (1997) was used for imaging the Quorn AMT apparent resistivity data while the seismic travel-time data were inverted using the scheme of Zelt and Barton (1998). The GEM inversions employed half-space staring models. Using various initial layered models, it was difficult to match the seismic data satisfactorily. We found it necessary to use the optimal resistivity model to guide the co-operative inversion of the seismic data for improved data matching.

Results and Model Interpretation

The resulting models that match our various data sets best are presented in Figures 4 to 6. The dc and AMT resistivities are in excellent agreement (see also Figure 6). The optimal seismic refraction model from co-operative inversion (Figure 7) shows similar subsurface structural features as the resistivity models suggesting that there may be a geological basis for correlating these models. The configuration of the boundary between the bedrock and its cover materials can be discerned in these models and is taken to be approximately marked by the 100 Ωm and 3000 m/s contours.

For the Quorn site, Meju et al (2003) observed that the resistivity (ρ in Ωm) and p-wave velocity (V_p in m/s) distributions (sampled at coincident grid positions or pixels in the 2D models) are related in the form (see **Figure 8**)

$$Log_{10}\,\rho = m\,Log_{10}\,V_p + c \qquad (1)$$

where the constants m and c respectively have values of 3.88 and -11 for the consolidated rocks (>3m deep) at this site (see trend B in Figure 8). An inverse relation was found to hold for the unconsolidated soil/drift deposits (i.e., top 3 m) for which m=-3.88 and c =13 (see trend A in Figure 8). It may be noted that *Rudman et al*., [1975, eq. 10] interrelated ρ_a and velocity logs from deep wells using an equation derived assuming ρ_a and V_p to be functions of porosity. Meju et al (2003) suggested that Rudman's equation simplifies to $Log_{10}\,\rho_a = (mLog_{10}\,V_p - mLog_{10}\,B)$ where m and B are empirical constants and is thus identical to Equation (1) determined experimentally relation for the consolidated rocks at Quorn. This would suggest that porosity is also a connecting factor for resistivity and velocity in the near-surface at Quorn.

Conclusions

This study has shown that 2-D imaging of collocated high-resolution seismic and geoelectromagnetic surveys can map the complex topography of the Mountsorrel granodiorite that forms the bedrock at Quorn. The structure of the overlying sedimentary materials was also resolved by the 2-D imaging surveys. A remarkable correlation was achieved between geoelectromagnetic and seismic models after co-operative inversion of seismic data incorporating the constraints furnished by resistivity models on lateral variations in the subsurface.

Acknowledgments

We thank Randy Mackie, Marcos Perez-Flores and Colin Zelt for permission to use their respective MT, dc resistivity and seismic codes.

References

Mackie, R., Rieven, S. and Rodi, **W.**, 1997, User manual and software for two-dimensional inversion of magnetotelluric data, Earth Resources Lab., Mass. Inst. of Technol., Cambridge.

Meju, M.A., Gallardo, L.A., and Mohamed, A.K., 2003. Evidence for correlation of electrical resistivity and seismic velocity in heterogeneous near-surface materials. *Geophys. Res. Lett*., **30 (7)**,1373-1376.

Meju, M.A., 2002. Geoelectromagnetic exploration for natural resources: models, case studies and challenges, *Surv*. *Geophys., 23*, 133-205.

Perez-Flores, M.A., Mendez-Delgado, S., and Gomez-Trevino, **E.,** 2001, Imaging low-frequency and dc electromagnetic fields using a simple linear approximation, *Geophysics*, 66, 1067-1081.

Rudman, A.J., Whaley, J.F., Blake, R.F.and Biggs, **M. E.,** 1975, Transformation of resistivity to pseudovelocity logs, *AAPG Bull.*, *59*, 1151-1165.

Sternberg, B.K., Washburne, J.C. and Pellerin, **L,** 1988, Correction for the static shift in magnetotellurics using transient electromagnetic soundings, *Geophysics, 53*, 1459-1468.

Zelt, C.A., and Barton, **P.J.,** 1998, Three-dimensional seismic refraction tomography: a comparison of two methods applied to data from the Faeroe Basin, *J. Geophys. Res., 103*, 7187-7210.

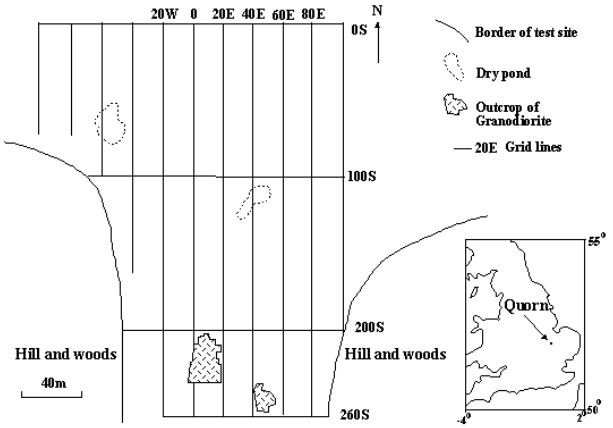

Figure 1. Map showing the geophysical survey grid at Quorn. The survey lines run N-S and are 20 m apart. Inset shows the location of Quorn in England.

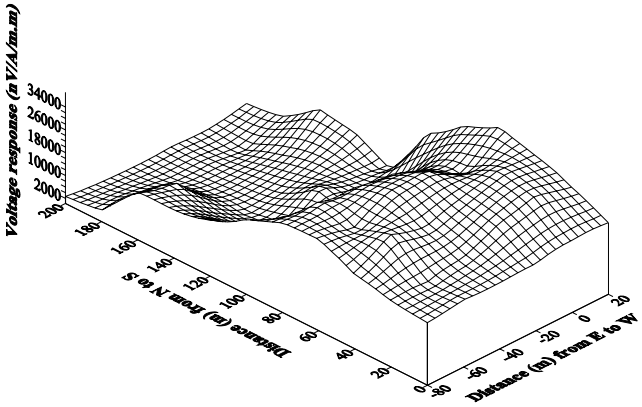

Figure 2a. 3-D veiw maps ofTEM voltage response at 0.016ms.

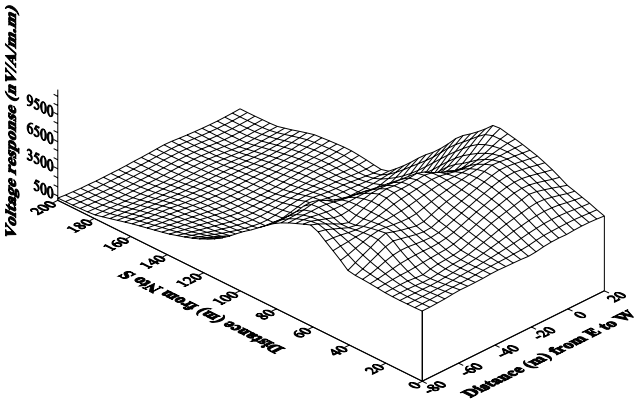

Figure 2c. 3-D veiw maps ofTEM voltage response at 0.0263 ms.

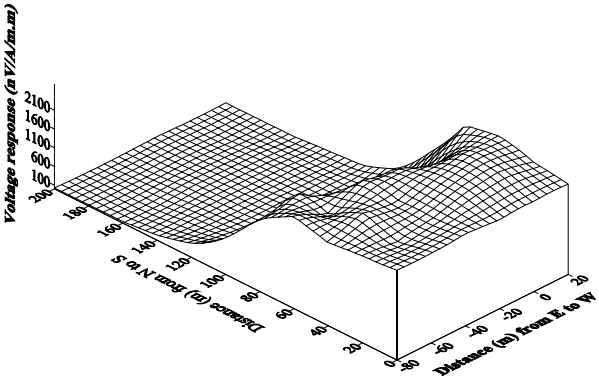

Figure 2c. 3-D veiw maps ofTEM voltage response at 0.0425ms.

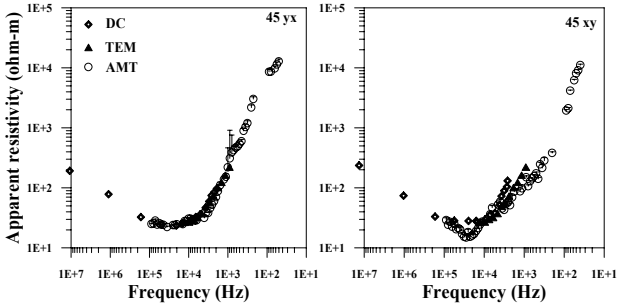

Figure 3. Example of TEM and bi-directional dc and AMT sounding curves from position 45S on line 20W. Shown are the north-south (xy) and east-west (yx) apparent resistivities.

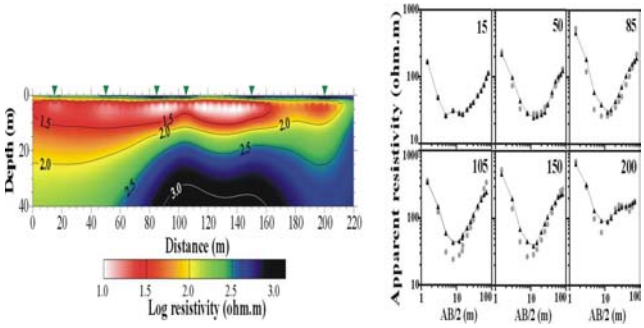

Figure 4. 2D resistivity model for line 20W. Shown are the optimal model (left plot) and the fit of the model responses (ornamented solid line) to field data (round symbols) at six sounding locations (right plot).

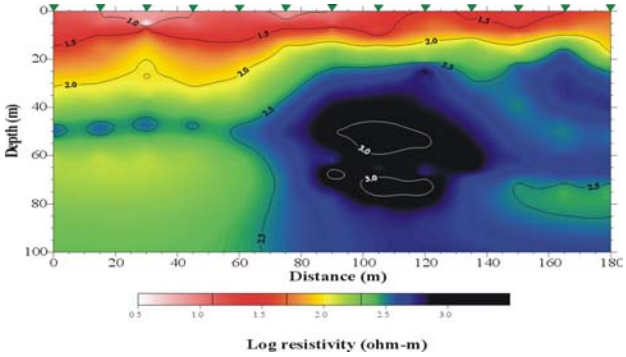

Figure 5. Optimal AMT resistivity model for line 20W. The 13 sounding positions (15m apart) are indicated at the top.

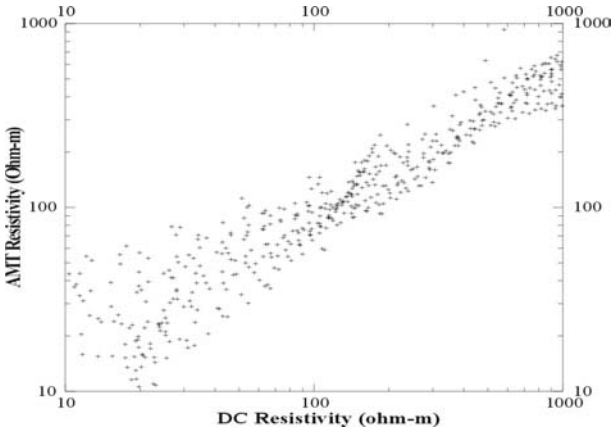

Figure 6. Comparison of dc and AMT resistivity imaging results. Samples are drawn from correspnding positions in the 2-D models for the top 40m of the subsurface.

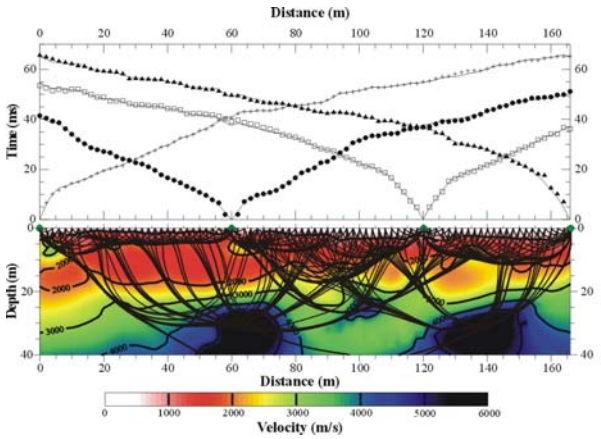

Figure 7. Optimal 2D velocity model for line 20W. The model is shown in the bottom diagram. The fit to the field recordings for different shot points (differentiated by symbols) is shown in the top plot.

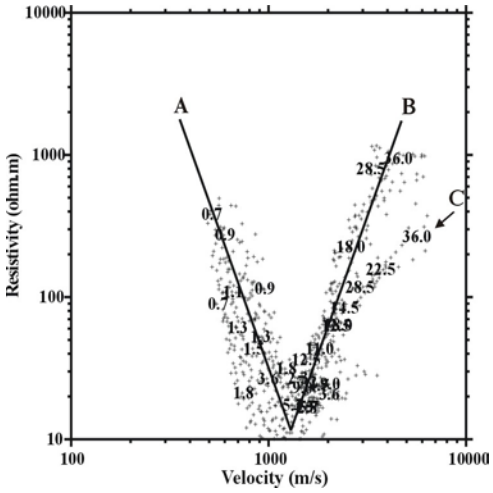

Figure 8. Relationship between logarithmic resistivity resistivity and seismic p-wave velocity on line 20W (Meju et al., 2003). The depth of sampling (in metres) is shown for selected points (pixels). Note the identified trends A and B of inverse slope. Trend B was constrained to pass through well estimated points thus giving less emphasis to contributions (e.g. zone C) from unresolved deep features in our seismic model.